Toward Accurate Environmental Mapping using Balloon-based UAVs

Ahmed Boubrima, Zhambyl Shaikhanov, Edward Knightly

Toward Accurate Environmental Mapping using Balloon-based UAVs

Ahmed Boubrima*†, Zhambyl Shaikhanov*, and Edward W. Knightly*
*Rice University, Texas, USA
†Univ Lyon, Inria, INSA Lyon, CITI, F-69621 Villeurbanne, France

***Abstract*— In this paper, we propose FloatSense, a novel balloon-based UAV network system for efficient and robust air pollution monitoring. Unlike prior related work commonly leveraging rotary-wing drones, FloatSense UAVs mainly exploit helium balloons to maintain elevation and use small lightweight normally-off fans as a propulsion mechanism. The proposed design enables as a result extended environmental sensing missions by staying afloat for weeks. However, the wind-dependent mobility nature of balloon systems involves multiple challenges in terms of system design and pollution mapping. We address in this paper the aforementioned challenges as we design and experimentally evaluate FloatSense in order to identify the benefits of the helium-powered flight mechanism on the accuracy of air pollution mapping compared to traditional rotatory-wing drones. We reveal that although balloon-based UAVs are prone to drifting off due to external forces like wind, FloatSense outperforms traditional drones even in the presence of considerable wind speeds. Moreover, we show that the wind-dependent balloon mobility nature also contributes to the performance improvement of FloatSense in air pollution monitoring missions.**

***Index Terms*— Unmanned aerial vehicles (UAV); balloon-based UAVs; rotatory-wing UAVs; environmental monitoring; air pollution mapping.**

I. Introduction

Environmental monitoring applications and mainly air pollution mapping (where the objective is to collect gas measurements that are used to interpolate air pollution maps) have been the focus of an increasing number of wireless sensing platforms in the last decade [1] [2]. Unmanned Aerial Vehicles (UAVs), also known as drones, are a vital part of air pollution mapping platforms due to their potential to increase both the spatial coverage and the spatial resolution of the monitored environment [3] [4]. Existing drone-based gas sensing platforms use traditional rotatory-wing UAVs that are equipped with large propellers, which allow them to hover at space points during the data collection process. Hovering is indeed required in order to cope with the relatively high response time of air pollution sensors. Nevertheless, the large propellers of traditional drones generate an undesired strong airflow that has a negative impact on the quality of gas sensing as demonstrated in multiple prior works [5] [6].

Using balloon systems to enhance aerial sensing: In order to eliminate the negative effects of large propellers on the sensing mechanism of gas sensors while still achieving the benefits of aerial sensing in terms of high spatial coverage and high spatial sensing frequency, we design a novel aerial pollution monitoring system, namely FloatSense, using balloon-based UAVs. In contrast to traditional rotatory-wing drones that require high propulsion power to maintain a stable elevation, balloons are usually filled with helium and are capable of flying due to the fact that helium is lighter than air [7] (hydrogen and methane can replace helium but are inflammable gases). As a result, balloon-based UAVs require minimal propulsion power to control their position. This is provided by a set of small fans that are normally off. Indeed, during the data collection process of gas concentrations, and as the drone is hovering, the fans are either completely turned off, or turned on in an intermittent way in the case of considerable wind speeds. As a result, this improves the balloon-based gas sensing accuracy compared to the performance of traditional rotatory-wing UAVs. The fans are also turned on to move the drone to a monitoring location not accessible by wind drift, or to return the drone to a desired landing location at the mission's conclusion. Moreover, the fans can rotate to change both azimuth and elevation positions.

Although the design key elements of FloatSense enable longer flight missions and are expected to reduce the negative effects of traditional drone propellers, the wind-dependent mobility nature of balloon systems involves multiple challenges in terms of (i) system design, and (ii) pollution mapping quality. Indeed, balloon-based UAVs are prone to easily drifting off in the presence of external forces such as wind gusts. We address in this paper the aforementioned challenges while proposing and experimentally validating our end-to-end gas-sensing balloon-based UAV network system.

A. Design of balloon-based gas sensing UAVs: Even though we have already addressed in our prior work [6] the effective design of traditional rotary-wing gas-sensing drones, the flight nature of balloon-based UAVs that rely on helium and small fans requires a design that incorporates unique balloon flight characteristics. Moreover, balloons' payload is minimal compared to traditional drones (over 1kg for medium-size hexacopters as shown in our prior work [6] vs. less than 50g for FloatSense UAVs). This, indeed, additionally limits the battery capacity and constrains the system power consumption.

Contribution: We, therefore, build the proposed FloatSense system while ensuring that gas sensors and fans are positioned on the helium-based balloons to provide both efficient sensing and propulsion. As a proof of concept, we use in our drone design a small-size foil-based balloon that inflates to 800mm

x 400mm (32in x 16in). The balloon is coupled with 3 fans that control both horizontal and vertical mobility and can also be used to return to the balloon launch site for a safe landing. For gas sensing, we embed Volatile Organic Compounds (VOC) sensors, which are widely used for tracking both industrial and traffic air pollution.

B. Balloon-based air pollution mapping quality: The higher accuracy of balloon-based point-wise gas sensing that is due to the mitigation of propellers' negative effects does not necessarily translate into an accurate overall air pollution mapping. Indeed, the quality of air pollution mapping (interpolation of collected gas measurements into a full map of pollution concentrations) depends on the spatial distribution of the most informative sensing locations where measurements need to be collected in order to interpolate pollution concentrations in the region of interest [8]. Moreover, the spatial distribution of optimal sensing locations (defined as the drone mission plan) is highly constrained by the power consumption model of the aerial sensing system, which is different in the case of FloatSense UAVs compared to traditional drones as the former is highly impacted by wind dynamics compared to the latter where they are much less pronounced.

Unfortunately, prior work on drone mission planning does not take into account the impact of the wind-dependent drone power consumption on the overall quality of environmental mapping, as the main focus in the literature is traditional rotatory-wing UAVs (i.e. wind-dependent mobility is assumed negligible in the literature) [6], [9]–[13].

Contribution: We first tackle the mission planning optimization problem while taking into account the wind-dependent mobility model of balloon systems. We then experimentally evaluate the performance of balloon-based UAVs for air pollution mapping while analyzing the mission planning results compared to traditional drones (using as a reference our prior work on rotary-wing drones [6]). The experimental results allow us to characterize the impact of the wind-dependent mobility nature of balloon-based UAVs on the optimization process of the most informative sensing locations. We reveal, in addition to other findings, that the performance improvement of balloon-based UAVs compared to traditional drones is not only due to the sensing accuracy improvement (non-presence of propellers) but is also related to the wind-dependent mobility of balloons.

Paper structure: The remainder of this paper is organized as follows. In Section II, we discuss the related work. Section III highlights our system design of FloatSense balloon-based UAVs. In Sections IV and V, we address the mission planning of balloon-based UAVs for air pollution mapping, and experimentally evaluate FloatSense compared to traditional drones. We finally conclude our paper in Section VI.

II. Related work

We highlight in this section the prior work that is related to our paper, which includes the areas of (i) aerial gas sensing and (ii) UAV mission planning.

A. Aerial Gas Sensing

Gas sensing can be performed using either (i) large-size and heavy sensors that provide high accuracy, or (ii) small-footprint and lightweight sensors that are less accurate than the first category. Due to their payload and power limitations, gas-sensing UAVs are rather equipped with lightweight sensors. The low accuracy of these lightweight sensors is due to the high impacts of weather conditions (wind, temperature, and humidity) on gas measurements [5].

Several literature works were focused on the evaluation of aerial gas sensing [5], [6], [14]–[16]. In these works, conventional rotatory-wing UAVs were considered in the experimental setups while authors focus mainly on analyzing the effects of propellers on the sensing quality of air pollution measurements.

As part of the aerial gas sensing accuracy analysis, some prior work performs multiple experimental flights in an urban area and then correlates drone measurements with the proximity to traffic sources [14]. This work showed the high noise level in pollution measurements and the need for a proper characterization of measurement errors. Other prior work proposes to characterize the airflow generated by the propellers of the drones and use the wind velocity level as a qualitative indicator of pollution measurements' errors [5] [15] [16]. In another recent work, authors infer the measurements' errors by co-locating drones and ground sensors and then extracting the correlations between pollution data and wind in addition to temperature and humidity [6].

B. UAV Mission Planning

UAV mission planning refers to the optimization process that allows drones to determine the most informative locations where they should collect their data in order to optimize the flight mission objective (for instance, optimizing the quality of gas maps that are generated/interpolated based on the collected data).

Mission planning of mobile sensors for environmental monitoring, in general, and air pollution mapping, in particular, has been extensively studied in the literature [9]–[13]. Most existing work relies on the spatial correlation of air pollution concentrations: that is, closer locations have a higher probability of being at the same concentration level [1], [17]–[19]. Based on that, the uncertainty of pollution estimation at unmeasured locations is formulated as a function of the spatial correlations of the measurements. The optimized sensing mission plan (i.e. the optimal set of sensing way-points) is then obtained by minimizing the uncertainty of pollution estimations at unmeasured locations.

C. Discussion

Unfortunately, prior work does not provide insights on the performance of balloon-based UAVs for environmental monitoring. Indeed, and contrary to conventional drones, balloons can be easily affected by moderate to high wind speeds.

Existing drone mission planning works don't take this into account as they are mainly designed for conventional UAVs where wind speed is assumed to have a negligible impact. To cope with that, we tackle in Section IV the mission planning optimization problem while taking into account the wind-dependent mobility of balloon systems.

III. System design of FloatSense UAVs

In order to focus on providing a proof-of-concept of the gas sensing application, we target experimental evaluations where wind speeds are less than 10 miles per hour as we build our UAV system using a small-size foil-based balloon that inflates to 800mm x 400mm (32in x 16in) as illustrated in Fig. 1. The balloon is coupled with 3 motorized fans that are placed underneath and control both the horizontal and vertical mobility of the UAV system. When filled with pure helium, our system can lift up to $40g$ payload while floating in the air for more than a week without any required propulsion power due to minimal helium leakage. As for steering the vehicle with the motorized fans, we pack a 2.4V 120mAh battery, which can run for up to 30 continuous minutes.

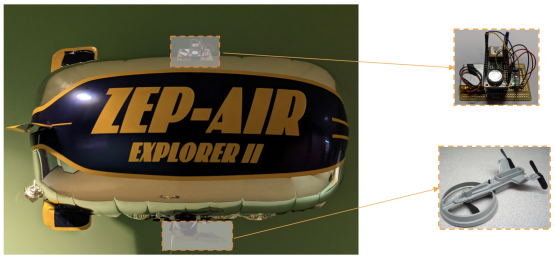

Fig. 1: FloatSense UAV System.

As illustrated in Fig. 1, the sensing, communication, and computation components of our system are mounted on top of the balloon in order to provide a balanced form. This allows us to provide both efficient sensing and propulsion. Moreover, we use light-weight and very-low-power components in order to meet the payload requirements of the helium balloon:

- In terms of computation, we employ a small footprint board that is based on the ATSAMD21G18 microcontroller.
- In terms of gas sensing, we employ a metal-oxide sensor developed by Bosch Sensortec to measure VOC concentrations that can provide a good signature of both industrial and traffic-related pollution emissions. The gas sensor chip has a response time of $8s$ and allows us also to measure temperature and humidity data.
- In terms of wireless communication between multiple UAV nodes, we employ low-power long-range LoRa radio modules (SX127x) that can operate at either 868 MHz or 915 MHz.

The sensing, communication, and computation components are powered using a 3.7v 500mAh battery, which allows our very-low-power system to run continuously for a week (or longer) depending on the sensing and communication frequency of gas concentrations.

IV. Mission planning of balloon-based UAVs

Balloon-based collected measurements are used to infer, by interpolation, air pollution maps over the region of interest. Therefore, the quality of these interpolated maps does not depend only on the accuracy of sensor data but also depends on the spatial distribution of measurement locations, which defines the UAV mission plan. Due to the wind-dependent mobility nature of balloon-based UAVs, prior work on traditional UAVs, where the impact of wind speed is assumed negligible, does not allow us at this point to determine the performance of balloon-based UAVs in terms of the overall air pollution mapping.

In this section, we tackle the mathematical fundamentals of UAV mission planning while incorporating the wind-dependent nature of the mobility of balloon-based UAVs. We then provide in the following section an experimental evaluation of our proposed mission planning approach while using experimental datasets collected using our balloon-based platform.

A. Objective and Main Notations

a) ***Region of interest****:* We approximate the region of interest using a vector $\boldsymbol{p}$ of l discrete points. **i.e.** $\boldsymbol{p} = [p_1, p_2, ..., p_l]^T$ where $p_i = (x_i, y_i, z_i)$. The ground truth air pollution concentrations (unknown values) that are associated with space $\boldsymbol{p}$ are denoted using $\boldsymbol{g} \in \mathbb{R}^l$. **i.e.** $\boldsymbol{g} = [g_1, g_2, ..., g_l]^T$ where g_i is the pollution concentration at point i.

b) ***Drone measurements****:* For presentation purposes, we first consider the case of a single drone and then extend this to consider a network of multiple drones. Let $\boldsymbol{z} \in \mathbb{R}^n$ denote the set of unknown measurements to be performed at a maximum of n different locations in space $\boldsymbol{p}$. Here, n depends on the power constraints of the drone system.

c) ***Objective****:* In air pollution mapping, drone measurements $\boldsymbol{z}$ are used to interpolate a vector $\boldsymbol{c} \in \mathbb{R}^l$, which is an estimation of $\boldsymbol{g}$. The objective of the mission planning process is therefore to find the optimal locations within space $\boldsymbol{p}$ where the measurements $\boldsymbol{z}$ should be collected in order to minimize the error of estimation of $\boldsymbol{g}$ by $\boldsymbol{c}$. Moreover, due to the limited power resources of drones, the mission planning process also optimizes the order in which sensing locations should be visited.

d) ***Decision variables****:* The main decision variables of the mission planning problem (locations of measurement locations and their visiting order) are represented using a matrix $H \in \mathbb{R}^{n \times l}$ where each matrix element h_{ij} is a Boolean set to 1 if measurement number i is performed at point j. Note that H is a matrix where the sum of each row is equal to 1.

Based on the definition of matrix H, the path that a drone should take during flight missions is determined by constraining the rows where the sum should be equal to 1 based on the distribution of pollution concentrations, and also constraining the order of columns where the sum is equal to 1 based on the power consumption of the drone system.

B. Optimization of Pollution Estimation

a) ***Formulation of pollution interpolation****:* Let the covariance matrix of pollution measurement errors of vector $\boldsymbol{z}$ be represented using matrix $R \in \mathbb{R}^{n \times n}$ while assuming that all gas sensors are properly calibrated prior to flight missions (i.e. measurement bias equal to 0). Assume also the availability of an estimation of pollution spatial correlations that are denoted using matrix $B \in \mathbb{R}^{l \times l}$, where each element b_{ij} reflects for space locations i and j the probability of being at the same concentration level [20].

In order to obtain the interpolated pollution vector $\boldsymbol{c} \in \mathbb{R}^l$ by interpolating pollution concentrations at unmeasured locations, the following matrix form is used:

$$\boldsymbol{c} = W\boldsymbol{z}, \tag{1}$$

where interpolation weights' matrix W is calculated as [21]:

$$W = BH^T(R + HBH^T)^{-1}, \tag{2}$$

and is a function of sensing errors' covariance matrix R and the spatial correlation matrix of pollution concentrations B.

b) ***Optimization of pollution interpolation****:* Let η_i denote the interpolated concentrations' errors with respect to the unknown ground truth value at each point i (i.e. $\boldsymbol{\eta} = \boldsymbol{c} - \boldsymbol{g}$). The covariance matrix of $\boldsymbol{\eta}$ (denoted F) is calculated as [21]:

$$F = (I_l - BH^T(R + HBH^T)^{-1}H)B, \tag{3}$$

where I_l is the identity matrix.

Based on the definition of matrix F, the optimization of the sensing locations where drones are sent to collect pollution measurements is obtained by minimizing

$$\sum_{i \in [1,l]} f_{ii}.$$

This allows determining in an optimal way the rows of matrix H where the sum should be equal to 1 in order to minimize the overall mapping error of the interpolated pollution map $\boldsymbol{c}$.

C. Mission Planning of Traditional UAVs

In order to provide a comparison baseline to the mission planning of balloon-based systems, we focus first on the case of traditional UAVs while assuming that the impact of the wind dynamics on traditional drones' speed is negligible (as in the literature).

In order to ensure that the optimal measurement locations are visited in an order that takes into account the flight power consumption of the traditional UAVs, the optimization of the matrix H is constrained by the following formula:

$$\sum_{k,i,j} h_{k,i} \cdot h_{k+1,j} \cdot T_{travel}(i,j) + \sum_{i,j} h_{i,j} \cdot T_{hover} \leq T_{flight}, \tag{4}$$

where T_{flight} is the maximum flight time of the drone, T_{hover} is the hover time that is required to perform gas sensing at each measurement location, and $T_{travel}(i,j)$ is the travel time between locations i and j based on the drone flight speed.

D. Wind-aware Mission Planning of Balloon-based UAVs

1) Balloon-based flight model: We assume that the propulsion mechanism of the drone system is powered separately from the sensing and communication components by using two different batteries (as in our proposed UAV system). We focus on optimizing the flight power consumption as the power consumption of flight motors is much higher than the consumption of sensing and communication components. Let MAX_{pow} be the capacity of the battery (maximum energy) that powers the propulsion mechanism of the drone system. Our optimal flight path is therefore constrained by MAX_{pow} as this impacts the selection of both sensing locations and their order.

Moreover, we assume that drones travel between measurement locations at a constant speed u. We also assume that the wind speed within the region of interest does not exceed the resistance threshold of the drones, which means that the drones' speed u can be maintained even when travelling upwind by adjusting the speed of the flight fans.

2) Wind speed and direction: For presentation purposes, we first focus on the case where wind speed and direction are constant within the region of interest during the relatively short time period of flight missions (the following formulations are extended later in this section to take into account variable wind). We denote the effective wind speed using $\vec{w}$, i.e. when the drone's fans are turned off, the drone flies following the direction of $\vec{w}$ at a speed equal to w. In order to determine $\vec{w}$ during flight missions, we propose to either access local data of weather stations or infer it using the internal accelerometer and gyroscope of the drone system while deactivating the drone fans during the inference process.

3) Wind-aware optimization of mission planning: Due to the nature of balloon-based UAVs, the wind speed and direction can have a high impact on the mobility of the drone system.

Let i and j be, respectively, the origin and destination locations at a given time during flight missions. Let $\overrightarrow{u_{ij}}$ be the drone's effective speed and direction vector as the drone is moving from location i to location j (we recall that $|\overrightarrow{u_{ij}}| = u$).

In order to ensure that the drone is moving accurately in the direction of j and at speed u, the generated drone propulsion power should be adjusted depending on the wind vector $\vec{w}$. Indeed, given $\vec{v}$ that denotes the drone fans' generated speed and direction vector, the relationship between $\vec{v}$, $\vec{w}$ and the drone effective speed and direction vector $\overrightarrow{u_{ij}}$ is defined as

$$\overrightarrow{u_{ij}} = \vec{w} + \vec{v}\,. \tag{5}$$

Based on (5), the energy consumption that is due to flying from point i to point j at speed u given a wind vector $\vec{w}$ is equal to

$$f_{pow}(|\overrightarrow{u_{ij}} - \vec{w}|) \cdot \frac{dist(i,j)}{u}, \tag{6}$$

where $dist$ is the Euclidean distance and f_{pow} is a known function that defines the drone-specific power consumption depending on the drone fans' generated speed $|\overrightarrow{u_{ij}} - \vec{w}|$.

Based on (6), we constrain the maximum energy consumption MAX_{pow} of each drone by the wind-dependent energy consumption when moving between every two locations i and j:

$$\sum_{k,i,j} h_{k,i} \cdot h_{k+1,j} \cdot f_{pow}(|\overrightarrow{u_{ij}} - \vec{w}|) \cdot \frac{dist(i,j)}{u} \leq MAX_{pow}. \quad (7)$$

Formula (7) impacts the optimal mission plan obtained in matrix H in two ways. First, given a configuration of sensing locations that minimize the pollution interpolation accuracy, Formula (7) ensures that the sensing locations are visited in an energy-efficient way by leveraging the dynamics of wind within the region of interest.

Moreover, and due to the joint optimization of both pollution estimation and wind-dependent flight power consumption, formula (7) also ensures that the selection process of sensing locations favours downwind locations whenever they offer similar interpolation performance compared to upwind locations (i.e. sensing locations are selected based on a joint combination of (i) pollution dynamics, and (ii) the effects of wind dynamics on drone mobility).

Case of non-constant wind vector: To take into account variable wind speed and direction, we extend Formula (7) by adding a time index to the wind vector, ensuring that the power consumption due to the wind-dependent mobility will be also time-dependent.

Case of balloons' network: To address the case of a network of multiple balloons, we extend decision variables h_{ij} with an additional index that defines the path plan of each balloon-based UAV individually in the optimization output.

V. Experimental Evaluation

In this section, we experimentally evaluate our mission planning method as we analyze the performance of the overall pollution mapping quality achieved by balloon-based UAVs compared to traditional drones. We use numerical solvers (CPLEX) to solve our optimization model of balloon-based UAV mission planning. This is motivated by the fact that our experimental evaluations were performed in regions of interest of medium size (less than $1km^2$). Nevertheless, and to scale to larger problem instances, the optimization formulation can also be solved on a step-by-step basis so that the number of decision variables is minimized in each mission planning iteration.

A. Data Collection Setup

In order to experimentally evaluate balloon-based air quality mapping, we collected an experimental dataset of co-located measurements of (i) FloatSense balloon-based UAVs, (ii) traditional drones (hexacopters designed in our prior work [6]) and (iii) reference ground sensors. We performed our dataset collection experiments in Houston, Texas during the months of September and October 2021 within two different industrial and residential neighbourhoods. The two neighbourhoods and their associated grid data collection points are illustrated in Fig. 2. Neighbourhood A (500m × 500m experiment area) is a residential neighbourhood mainly exposed to urban traffic pollution while Neighborhood B (1000m × 1000m experiment area) is an industrial neighbourhood that is exposed to the high activity of multiple chemical plants. In addition to our pollution data sets, and in order to assess the impact of wind-dependent balloon mobility, we also used wind data sets that are provided by local weather stations.

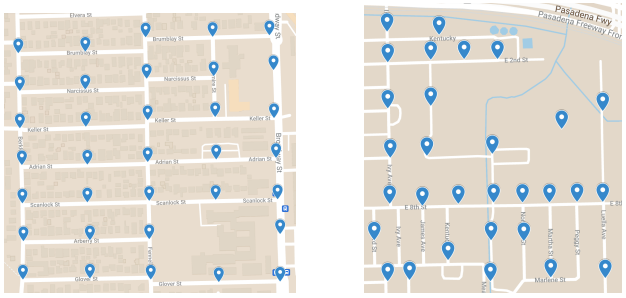

(a) Neighborhood A (500m × 500m)

(b) Neighborhood B (1km × 1km)

Fig. 2: Regions of Interest used in our experiments.

B. Obtained Dataset

Before evaluating the air pollution mapping performance of balloon-based UAVs, we first analyze the spatial characteristics of the collected dataset as we depict in Fig. 3 the spatial autocorrelation function of the collected pollution maps.

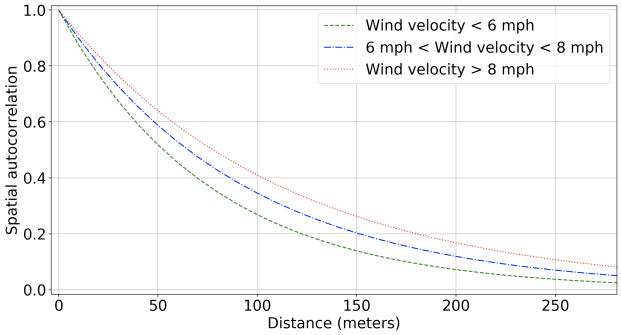

Fig. 3: Spatial autocorrelation of reference concentrations.

Fig. 3 highlights, as expected, the intrinsic spatial correlation between sensing locations as a function of distance. Most importantly, Fig. 3 shows that higher wind speeds within our regions of interest lead to better spatial correlation. This is mainly due to the spatial distribution of pollution sources and the fact that our regions of interest have a relatively small size of less than 1000m x 1000m.

Moreover, we also analyze the distribution of the variability of pollution concentrations within our regions of interest during the data collection time periods. Fig. 4 depicts the histogram of the variance of the collected maps and shows that our dataset has a uniformly distributed variance. This allows us indeed to consider later in this section the impact of

pollution variability on the air pollution mapping performance of balloon-based UAVs compared to traditional drones.

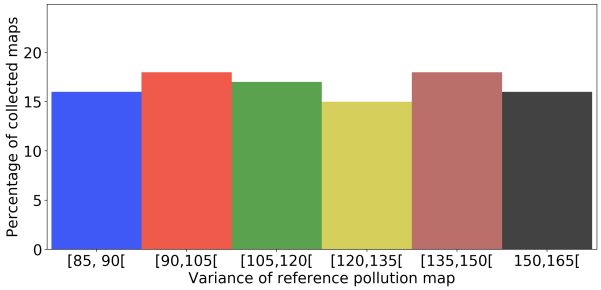

Fig. 4: Distribution of the pollution variability of collected reference maps.

C. Flight Power Consumption

In order to provide a fair experimental comparison between balloon-based UAVs and traditional drones, we assume that both aerial systems travel between measurement locations at the same speed that we set at $5m/s$. Although traditional drones might seem faster in practice, balloon-based UAVs can actually still be as fast depending on their size and the amount of helium they contain. However, the power consumption that is due to fly at that common $5m/s$ is wind-dependent in the case of balloon-based UAVs compared to traditional drones.

Moreover, we assume that, by default, both aerial systems are capable of the same payload (i.e. by default, they are equipped with the same battery capacity). Note that the overall flight time of the two aerial systems can still be different though as the power consumption required to fly the balloon-based UAV is wind-dependent.

D. Evaluation Metric and Baseline

We evaluate the air pollution mapping quality of both aerial systems by running the corresponding mission planning approach. While evaluating the performance of each one of the aerial systems, we use the corresponding collected measurements to perform the interpolation process and hence obtain an estimation of ground truth concentrations.

We consider as a theoretical baseline the mission planning results that can be obtained with the balloon system given a perfect knowledge of the distribution of pollution concentrations (i.e. by assuming a perfect knowledge of the not-yet-measured locations during the mission planning process). We refer to this baseline in what follows by the theoretical lower bound.

In order to quantify the quality of the interpolation provided by each system and the proposed baseline, we use as a performance metric the relative mean squared error (RMSE) of the interpolated map with respect to the map collected using reference ground sensors.

E. Experimental Results

1) First performance comparison scenario: In order to assess the overall mapping performance provided by the two aerial sensing systems, we vary the battery budget of both balloon-based UAVs and traditional drones as we evaluate the RMSE of the interpolation maps resulting from optimal mission plans.

Due to the nature of wind-dependent balloon-based UAVs, the initial location of both systems in the region of interest is set to the corner of the map that allows the balloon system to maximize down-wind flights. This is usually the case in practice as launching the balloon system from a different location would result in unnecessary energy consumption. The obtained results corresponding to our 30 collected pollution datasets are averaged and depicted in Fig. 5.

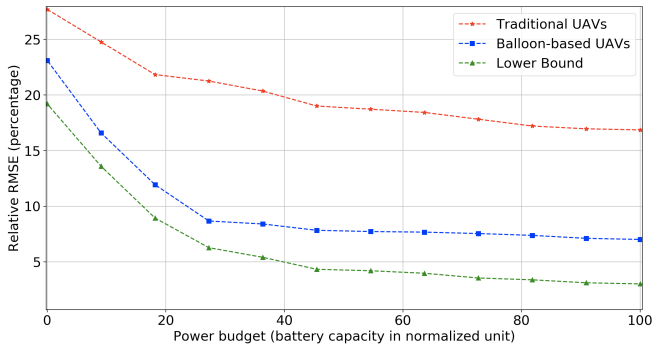

Fig. 5: Air pollution mapping performance of FloatSense UAVs compared to traditional drones.

First, the results in Fig. 5 show that the air pollution mapping error corresponding to balloon-based UAVs is lower than what is achieved using traditional rotatory-wing UAVs assuming that both systems are provided with the same power budget. The performance difference between the two systems is noticeable even for low power budgets as balloon-based UAVs outperform the traditional UAVs by at least a factor of 3 with respect to the theoretical lower bound. This result shows that the sensing accuracy improvement of balloon-based UAVs over traditional drones has been maintained in the mission planning process and highlights therefore that the balloon system is power efficient in terms of leveraging the effects of wind dynamics on balloon mobility. Indeed, Fig. 5 shows that the balloon system appears to undergo two phases during the flight missions: the first phase ends at about 25 normalized energy units and is characterized by a faster-decreasing evolution compared to the following second phase where the ratio between performance improvement and power consumption appears to be much less pronounced. The reason behind the existence of these two phases is actually the way the balloon system takes advantage of the wind speed and direction' dynamics. Indeed, during the first phase, the balloon-based UAV travels mainly downwind which results in minimal power consumption compared to the second phase where the balloon system travels mostly upwind as it finally reaches the side of the map that is opposite to where it was launched.

2) Impact of drone battery payload and wind dynamics: Note that the improvement factor obtained so far is achieved

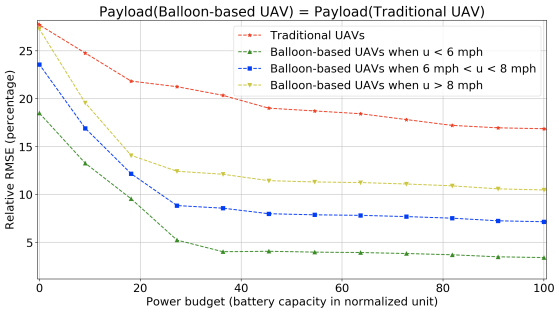

(a) Payload(Balloon UAV) = Payload(Traditional UAV)

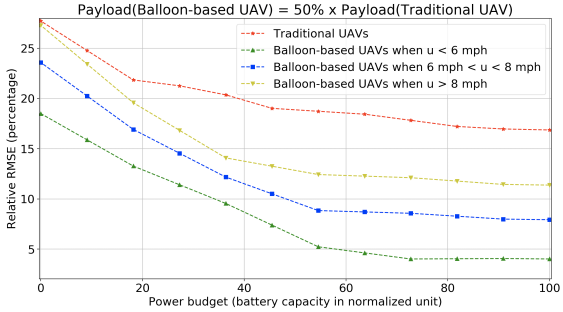

(b) Payload(Balloon UAV) = 50% x Payload(Traditional UAV)

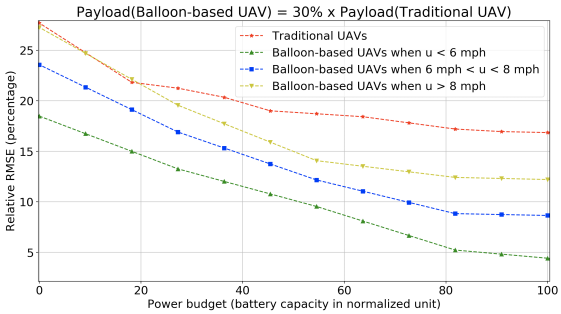

(c) Payload(Balloon UAV) = 30% x Payload(Traditional UAV)

Fig. 6: Air pollution mapping performance depending on wind velocity and maximum balloon payload.

while assuming that both the traditional drone and the balloon-based UAV have the same payload (same maximum battery capacity). However, traditional drones are capable in practice of carrying larger batteries in general. We, therefore, evaluate in what follows the impact of the maximum payload of the balloon system compared to traditional drones while also identifying the effects of the wind-dependent mobility of balloons. We depict in Fig. 6 the resulting air pollution mapping performance depending on the wind speed that is observed in our regions of interest while considering 3 scenarios regarding the maximum battery payload of the balloon system. Mainly, we average for each payload scenario the pollution mapping performance that is achieved by the balloon-based UAV system while separating the data sets into 3 groups in function of the wind velocity: less than 6 miles per hour, between 6 and 8 miles per hour, and finally over 8 miles per hour.

In terms of the effects of the balloon maximum payload, Fig. 6 does show that the performance improvement achieved in the previous results drops as the traditional drone system is equipped with larger batteries compared to the balloon. Indeed, the performance improvement factor with respect to the theoretical lower bound drops to less than 1.5 when traditional drones are equipped with more than 3 times larger batteries. Therefore, in a real-life scenario, balloon-based UAVs need to be equipped with large enough batteries to ensure a better performance compared to traditional drones. This can be achieved by using larger balloons that are filled with more helium to increase their maximum payload while maintaining their power efficiency during the data collection hovering time.

Furthermore, the results in Fig. 6 show that the higher the wind speed, the lower the pollution mapping performance. This is indeed due to the fact that higher wind speeds have a negative impact on balloon-based sensing accuracy. Nevertheless, Note that higher wind speeds also allow the balloon-based UAV system to reduce its power consumption when travelling downwind, but this appears to have less impact on the performance results compared to lower wind speeds.

Moreover, Fig. 6 also emphasizes the impact of wind velocity on the mission flights and their two phases of operation that we identified in the previous Fig. 5. Indeed, we observe in Fig. 6 that wind speeds that are higher than $8mph$ appear to accelerate the downwind travel phase (which ends with less than 20 normalized energy units) while wind speeds that are lower than $6mph$ appear to extend this first phase of flight missions (which takes more than 30 normalized energy units as opposed to the average value of 25 units that we observed earlier). This fact means that the performance improvement in the presence of lower wind speeds is not only due to the sensing accuracy improvement but is also jointly dependent upon the wind-dependent mobility nature of balloon-based UAVs.

3) Impact of pollution variability: In addition to the impact of the drone payload and the wind dynamics, we also assess the performance of the balloon-based UAVs depending on the variability of pollution concentrations within our regions of interest. Based on our previous dataset analysis in Fig. 4, we classify our dataset maps into 3 groups: high pollution

variability where the variance of reference concentrations is higher than $135ppb^2$, low pollution variability where the variance is lower than $105ppb^2$ and finally average pollution variability within the remaining variance interval. In all three scenarios, we assess the improvement factor of balloon-based UAVs over traditional drones using the default evaluation parameters. We report the obtained results in Fig. 7 while highlighting the performance improvement factor achieved at the initial stage (20%), mid-stage (50%) and final stage (80%) of the drone missions.

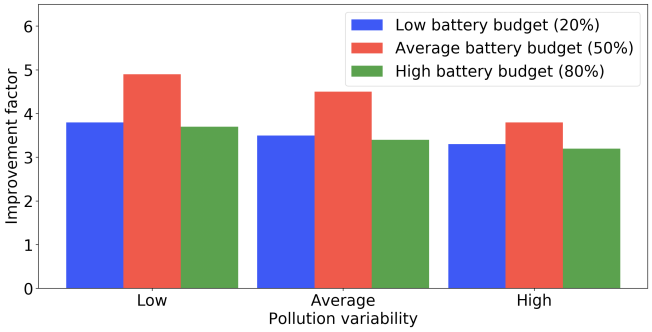

Fig. 7: Mapping performance vs. pollution variability.

Fig. 7 shows that the performance improvement achieved at the final stage of the drone missions is overall maintained and only decreases slightly (less than 0.3) when the pollution variability increases. This is indeed due to the fact that sensing errors are accentuated in the interpolation process of pollution mapping in the presence of high pollution variability, and this is the case for both traditional and balloon-based UAVs.

Furthermore, Fig. 7 also shows that the wind-dependent balloon mobility is altered depending on the variability of pollution concentrations. Indeed, in the presence of high pollution variability, we observe that the change in the performance improvement from early stage to mid-stage, and from mid-stage to final stage is much less pronounced compared to the two scenarios of low and average pollution variability. This is indeed due to the fact that the balloon upwind mobility is much more used in the case of high pollution variability, which requires the balloon system to collect dense measurements compared to the case of low pollution variability.

VI. Conclusion

Unmanned Aerial Vehicles (UAVs), also known as drones, are a vital part of air pollution mapping platforms. Unlike existing drone-based gas-sensing platforms that use traditional rotatory-wing UAVs, we propose and validate in this paper the first end-to-end gas-sensing balloon-based UAV network system by addressing the design of balloon-based gas-sensing UAVs, and the characterization of the sensing and mapping quality of balloon-based UAVs compared to traditional drones. We show that balloon-based UAVs outperform traditional drones even in the presence of considerable wind speeds. We also show that the wind-dependent balloon mobility nature also contributes to the performance improvement of balloon-based UAVs.

References

[1] D. Hasenfratz, O. Saukh, C. Walser, C. Hueglin, M. Fierz, and L. Thiele, "Pushing the spatio-temporal resolution limit of urban air pollution maps," in *Pervasive Computing and Communications (PerCom), 2014 IEEE International Conference on*. IEEE, 2014, pp. 69–77.

[2] A. Anjomshoaa, F. Duarte, D. Rennings, T. J. Matarazzo, P. deSouza, and C. Ratti, "City scanner: Building and scheduling a mobile sensing platform for smart city services," *IEEE Internet of Things Journal*, vol. 5, no. 6, pp. 4567–4579, 2018.

[3] D. Bhattacharya, S. Misra, N. Pathak, and A. Mukherjee, "Idea: Iot-based autonomous aerial demarcation and path planning for precision agriculture with uavs," *ACM Transactions on Internet of Things*, vol. 1, no. 3, pp. 1–21, 2020.

[4] H. Shakhatreh, A. H. Sawalmeh, A. Al-Fuqaha, Z. Dou, E. Almaita, I. Khalil, N. S. Othman, A. Khreishah, and M. Guizani, "Unmanned aerial vehicles (uavs): A survey on civil applications and key research challenges," *IEEE Access*, vol. 7, pp. 48 572–48 634, 2019.

[5] P. P. Neumann, "Gas source localization and gas distribution mapping with a micro-drone," 2013.

[6] A. Boubrima and E. W. Knightly, "Robust environmental sensing using uavs," *ACM Transactions on Internet of Things*, vol. 2, no. 4, pp. 1–20, 2021.

[7] S. Kuznetsov, G. N. Davis, E. Paulos, M. D. Gross, and J. C. Cheung, "Red balloon, green balloon, sensors in the sky," in *Proceedings of the 13th international conference on Ubiquitous computing*, 2011, pp. 237–246.

[8] T. Cabreira, L. Brisolara, and P. R Ferreira, "Survey on coverage path planning with unmanned aerial vehicles," *Drones*, vol. 3, no. 1, p. 4, 2019.

[9] A. Belkhiri, W. Bechkit, and H. Rivano, "Virtual forces based uav fleet mobility models for air pollution monitoring," in *2018 IEEE 43rd Conference on Local Computer Networks (LCN)*. IEEE, 2018, pp. 481–484.

[10] A. Krause, C. Guestrin, A. Gupta, and J. Kleinberg, "Robust sensor placements at informative and communication-efficient locations," *ACM Transactions on Sensor Networks (TOSN)*, vol. 7, no. 4, p. 31, 2011.

[11] Y. Xiang, L. S. Bai, R. Pledrahita, R. P. Dick, Q. Lv, M. Hannigan, and L. Shang, "Collaborative calibration and sensor placement for mobile sensor networks," in *2012 ACM/IEEE 11th International Conference on Information Processing in Sensor Networks (IPSN)*. IEEE, 2012, pp. 73–83.

[12] Y. Yang, Z. Zheng, K. Bian, L. Song, and Z. Han, "Real-time profiling of fine-grained air quality index distribution using uav sensing," *IEEE Internet of Things Journal*, vol. 5, no. 1, pp. 186–198, 2017.

[13] B. Zhang, T. Xi, X. Gong, and W. Wang, "Mutual information maximization-based collaborative data collection with calibration constraint," *IEEE Access*, vol. 7, pp. 21 188–21 200, 2019.

[14] Q. Gu, D. R Michanowicz, and C. Jia, "Developing a modular unmanned aerial vehicle (uav) platform for air pollution profiling," *Sensors*, vol. 18, no. 12, p. 4363, 2018.

[15] J. J. Roldán, G. Joossen, D. Sanz, J. Del Cerro, and A. Barrientos, "Mini-uav based sensory system for measuring environmental variables in greenhouses," *Sensors*, vol. 15, no. 2, pp. 3334–3350, 2015.

[16] T. F. Villa, F. Salimi, K. Morton, L. Morawska, and F. Gonzalez, "Development and validation of a uav based system for air pollution measurements," *Sensors*, vol. 16, no. 12, p. 2202, 2016.

[17] A. Boubrima, W. Bechkit, and H. Rivano, "On the deployment of wireless sensor networks for air quality mapping: Optimization models and algorithms," *IEEE/ACM Transactions on Networking*, vol. 27, no. 4, pp. 1629–1642, 2019.

[18] G. Hoek, R. Beelen, K. De Hoogh, D. Vienneau, J. Gulliver, P. Fischer, and D. Briggs, "A review of land-use regression models to assess spatial variation of outdoor air pollution," *Atmospheric environment*, vol. 42, no. 33, pp. 7561–7578, 2008.

[19] V. Roy, A. Simonetto, and G. Leus, "Spatio-temporal sensor management for environmental field estimation," *Signal Processing*, vol. 128, pp. 369–381, 2016.

[20] D. W. Wong, L. Yuan, and S. A. Perlin, "Comparison of spatial interpolation methods for the estimation of air quality data," *Journal of Exposure Science and Environmental Epidemiology*, vol. 14, no. 5, pp. 404–415, 2004.

[21] E. Kalnay, *Atmospheric modeling, data assimilation and predictability*. Cambridge university press, 2003.